Characterisation of an ultrasonic sensor designed to identify reflectors in 3D environments.

Jiménez J.A., Ureña J., Mazo M., Santiso E, Hernández A., Meca F.J..

Department of Electronics of the University of Alcalá.
Carretera Madrid-Barcelona Km. 33.600. Campus Universitario
28871 Alcalá de Henarés (Madrid)
jimenez@depeca.uah.es

Abstract

This paper presents an ultrasonic sensor made up of several transducers located on various different horizontal planes, designed for navigation and localisation applications in the mobile robot (MR) field. The sensor proposed is equipped with an emitter and nine receivers. The times-of-flight (TOF) provided by the transducers enable the two types of basic reflectors (planes and edges) to be classified. The system may be easily extended to include two emitters and fourteen receivers in order to identify corners. Optimal classification of the reflectors will facilitate both localisation of the mobile robot and the generation of environment maps that are useful for navigation tasks. The innovation with this sensor as regards prior papers in this field lies in the high degree of redundancy that it provides, which greatly facilitates the detection of erroneous measurements caused by false reflections, and in the simplicity of the classification algorithm used, which gives it a low computational load.

1. Introduction

The use of ultrasonic sensors to both generate environment maps and classify basic reflectors (planes, edges and corners) is justified by their low cost, small size, low consumption and simple signal processing requirements, which facilitate operations in real time. However, they are not without their disadvantages. They have several drawbacks, among which are poor angular resolution, specular reflections, cross-talk when various transducers emit simultaneously and their sensitivity to environment variables such as temperature and humidity.

For many years, researchers have worked on papers aimed at compensating for these drawbacks. As a result, to resolve the problem of the angular resolution sensor configurations are used that are made up of various transducers, at least one emitter and two receivers. In this way it is possible not only to ascertain the distance to the reflector, but also the listening angle [1,2].

As far as the specular reflections are concerned, the only way of correcting their effects is to combine the redundant information provided by the sensor system at that or various different moments. Various different techniques may be used to combine the information, such as probabilistic techniques based on Bayesian theory [3,4], which is perhaps the most used, or techniques based on theory of evidence (Dempster-Shafer) [5], fuzzy maps [6] and neural networks [7]. Comparisons of the various combination techniques may be found in [8]. Techniques have also been developed based on pulse encoding that enables simultaneous emission to take place and avoids cross-talk [9].

The majority of research related to the application or use of ultrasonic sensors has two basic objectives: the generation of environment maps and the classification of basic reflectors (edges, planes and corners) that are easily found in the environments in which the robot is to carry out its activity, and that will be used as natural landmarks in localisation tasks. This paper concentrates its analysis on the usefulness of ultrasonic sensors for basic reflector classification tasks.

Two techniques are generally used to perform basic reflector classification: that based on measuring the time-of-flight (TOF) [1], and that based on comparing the amplitude of the echoes received from the different types of reflector [10]. The methods based solely on comparing the amplitude are reasonably fast and only require simple hardware and software. However, the fluctuations suffered by the amplitude of the acoustic signals due to variations in temperature and humidity, air currents, distance and even the absorbency of the surfaces, makes them less recommendable. Other papers have been written in which amplitude information and TOF have been combined [11].

All of the previous papers perform basic reflector classification in 2D. However, there are a number of reasons that justify performing three-dimensional reflector classification.

- In order to obtain an accurate representation of the environment it is necessary to have three-dimensional primitives (planes, corners, three-dimensional edges), especially given the fact that the robot moves in a three-dimensional environment. The reflectors are not all located on the same plane. However, when 2D is used the error is committed of assuming that all of the reflectors are located on the same plane.
- Indoor environments contain numerous three-dimensional natural landmarks such as walls and intersections between the wall and floor and wall and ceiling which may be used for localisation tasks. Therefore, it is useful if the robot is able to distinguish and classify this type of reflector.

There are very few papers dealing with the classification of three-dimensional objects using ultrasonic sensors applied to localisation and navigation tasks in MR's . Those worth highlighting are [12,13].

Various papers have been written on recognising three-dimensional objects in classification tasks, one of which is [14], in which an array of transducers made up of 8*8 elements is used to classify various types of object by applying holographic techniques and a neural network. In [15], techniques based on acoustic holography are also used to recognise the outline of 3D objects. In [16], a complex ultrasonic vision system designed to classify basic objects (polished glass surfaces, corners and spheres) is described. The techniques developed in these three papers require complex calculations and *a priori* knowledge bases, which make them difficult to adapt to applications related to navigation and localisation in MR's.

This paper presents a sensor made up of nine transducers able to discriminate between planes and edges using a single ultrasonic emission and a classification algorithm of extremely low computational load. It is also worth highlighting the high level of redundancy that it provides, which facilitates identification of erroneous measurements caused by false reflections.

The paper is structured in the following manner: section 2 describes the architecture of the proposed sensor; section 3 comments briefly on the technique used to achieve simultaneous emission and to identify the echoes by origin when various emitters are used. Section 4 presents the algorithm used to carry out classification. Section 5 presents the results obtained using the described classification algorithm. The final section comments on the lines of research that are currently being worked on.

2. Sensor structure.

In order to obtain the minimum number of transducers needed to detect the two basic reflector types (edges and planes) it is assumed that the surfaces are specular, given that their roughness is low compared to the wavelengths of the ultrasonic signals employed. As a result of this assumption, it is possible to ascertain the behaviour of each transducer for each type of reflector using a geometric approach. The transmitters are replaced by their virtual image so that the time-of-flight or distance from a transmitter to a receiver will be equal to the distance between the receiver and the virtual image of the transmitter.

Taking these considerations into account, in [1,17] it is established that to carry out classification of the three basic reflector types (corners, planes and edges) in 2D environments at least two emiters and two receivers are required. Using a single ultrasonic emission it will only be possible to classify between edge-type reflectors and the rest (planes and/or corners). Using measurements obtained from different positions it would be possible to discriminate between planes and corners. However, this would also entail the need for accurate positioning. It would also be possible to make two consecutive emissions from the same position, but this has the drawback of restricting the speed of the MR. Techniques currently exist that enable various transducers to make simultaneous emissions without generating cross-talk. One of these is introduced in section 3.

In [12] it is demonstrated that at least three transducers are needed to classify three-dimensional reflectors. In this case the three transducers are distributed in the shape of a equilateral triangle. An MLE (Maximum Likelihood Estimator) is used to carry out classification of the different reflector types.

The structure presented in this paper (figure 1) represents an advance on that presented in [12] in two basic aspects: on the one hand, it enables a high number of measurements to be obtained simultaneously, which provides a high level of redundancy that facilitates the identification of erroneous measurements, and, on the other, the classification algorithm is much simpler, which results in a much lower computational load and shorter calculation time.

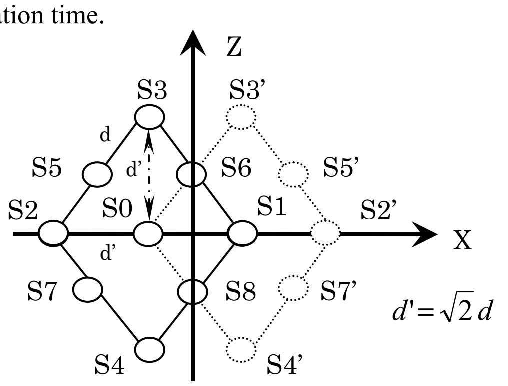

Fig. 1. Sensor structure.

As may be observed in figure 1, the transducers have been distributed in a rhombus shape, this structure has been chosen, among other reasons, for its symmetry as, in this way, the calculations are simplified, the sensor is unaffected by rotations and it is possible to add further transducers easily if necessary.

Sensor is make up by two rhombus, first (continuous line in figure 1, transducers S0 to S8) form basic structure to discriminate between edges and planes/corners. In this case, S0 acts as emitter/receiver whilst S1 to S8 act as receivers. Transducers S2' to S7' (discontinuous line in figure 1) are appended to basic structure when besides is desired to realize other classification between planes and corners. In this latter case, the emission of ultrasonic signals by the two emitter transducers S0 and S1, would be carried out simultaneously using the technique described in [18].

The distance *d* has been set at 20 centimetres as a compromise solution that attempts to balance the problem of echo correspondence [17] with the discrimination capacity of the sensor that depends greatly on the separation distance between transducers.

3. Simultaneous emission and echo discrimination by origin.

The possibility of using Golay complementary sequence pairs to determine TOFs has been demonstrated in previous works [9]. In order to allow the discrimination of echoes depending on the source of emission, there is a low-level electronic system in each receptor for the detection of two different and orthogonal Golay sequence pairs (see Fig. 2). Here it can be observed the block diagram for the emitter/receiver 1: its emission is coded by the pair [A_1, B_1], and it discriminates echoes from itself or from other emitter (wich emission was coded by the pair [A_2, B_2]). This system can be seen in [18].

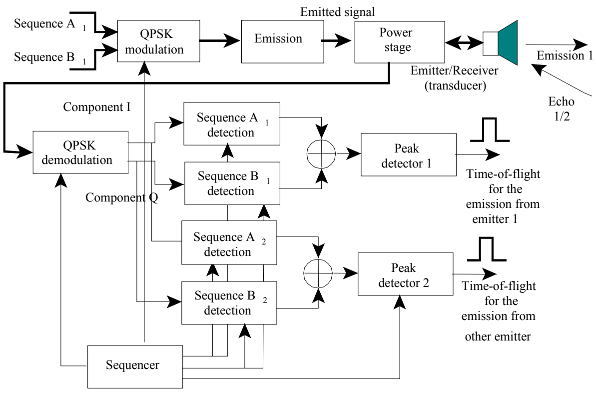

Fig. 2. Simplified scheme of processing system in a emitter/receiver transducer

4. Classification algorithm.

The algorithm presented is a 3D extension of the proposals developed in other papers on the same line of research for bi-dimensional environments [17] and concentrates on analysis of discrimination between edges and planes using a single ultrasonic signal emission.

The classification algorithm is based on obtaining the geometric distance ratios (r_i with $0 \le i \le 8$) between the various receiver transducers and the reflector under study for both planes and edges.

Once these geometric ratios have been obtained, the distances are determined according to the times-of-flight, taking into account that when the reflector is a plane, it may be assumed that the emitter is the virtual image of the same (figure 3), which means that the ratio between the distance to the reflector and the times-of-flight will be determined by the following expression, assuming that, as is the case in this instance, the emitting transducer is S0 and the receivers are S_j ($0 \le j \le 8$) :

$$r_{0j} = c\, t_{0j} \qquad (1)$$

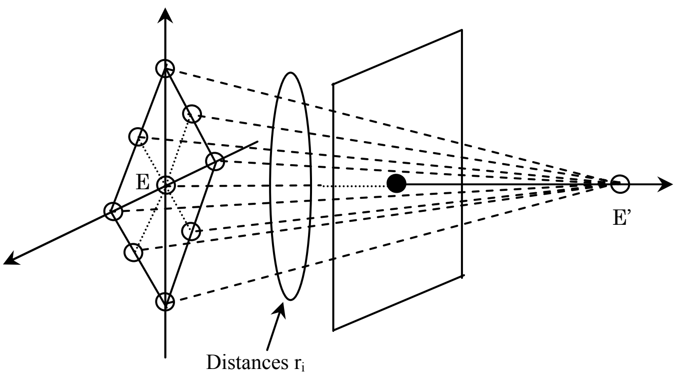

Fig. 3. Times-of-flight and virtual image for plane-type reflectors.

When the reflector is an edge (figure 4), the distance travelled by an echo emitted by emitter 0 and received by receiver *j* is the sum of the distance from this transmitter to the edge plus the distance from the edge to the emitter. Therefore, the ratio between the distance from the receiver transducer to the reflector and the corresponding time-of-flight will be determined by the following expression:

$$r_{0j} = c\,(t_{0j} - \frac{t_{00}}{2}) \qquad (2)$$

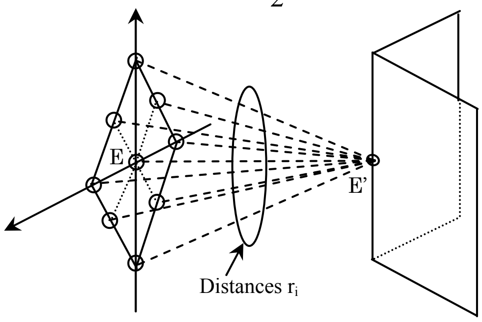

Fig. 4. Times-of-flight for edge-type reflectors.

Being c, in the two earlier expressions, the velocity of the sound.

On the basis of these considerations, the geometric ratios are obtained according to the distances r_i. Generalising for the case of three transducers located at the co-ordinates (x_n, y_n, z_n), (x_{n+1}, y_{n+1}, z_{n+1}) and (x_{n+2}, y_{n+2}, z_{n+2}) and a reflector located at the co-ordinates (x_p, y_p, z_p), the distances from each transducer to the reflector, independently of type of reflector involved, are given by:

$$x_p^2 + y_p^2 + z_p^2 - 2x_p x_n - 2z_p z_n + x_n^2 + z_n^2 = r_n^2 \qquad (3)$$

$$x_p^2 + y_p^2 + z_p^2 - 2x_p x_{n+1} - 2z_p z_{n+1} + x_{n+1}^2 + z_{n+1}^2 = r_{n+1}^2 \qquad (4)$$

$$x_p^2 + y_p^2 + z_p^2 - 2x_p x_{n+2} - 2z_p z_{n+2} + x_{n+2}^2 + z_{n+2}^2 = r_{n+2}^2 \qquad (5)$$

Subtracting expressions 3-4 and 3-5 produces expressions 6 and 7 respectively:

$$2x_p(x_{n+1} - x_n) + 2z_p(z_{n+1} - z_n) + x_n^2 - x_{n+1}^2 + z_n^2 - z_{n+1}^2 = r_n^2 - r_{n+1}^2 \qquad (6)$$

$$2x_p(x_{n+2} - x_n) + 2z_p(z_{n+2} - z_n) + x_n^2 - x_{n+2}^2 + z_n^2 - z_{n+2}^2 = r_n^2 - r_{n+2}^2 \qquad (7)$$

From expressions 6 and 7 it is possible to obtain x_p:

$$x_p = \frac{r_n^2 - r_{n+1}^2 - x_n^2 + x_{n+1}^2 + z_{n+1}^2 - z_n^2 - 2z_p(z_{n+1} - z_n)}{2(x_{n+1} - x_n)} \qquad (8)$$

$$x_p = \frac{r_n^2 - r_{n+2}^2 - x_n^2 + x_{n+2}^2 + z_{n+2}^2 - z_n^2 - 2z_p(z_{n+2} - z_n)}{2(x_{n+2} - x_n)} \qquad (9)$$

Equalling expressions 8 and 9 and, in the case that the three transducers considered (x_n, x_{n+1} and x_{n+2}) were to be located on the same line segment, expression 10 is obtained.

$$a_1 r_n^2 - b_1 r_{n+1}^2 + c_1 r_{n+2}^2 = d_1 + e_1 \qquad (10)$$

being

$$a_1 = (x_{n+2} - x_{n+1})$$
$$b_1 = (x_{n+2} - x_n)$$
$$c_1 = (x_{n+1} - x_n)$$
$$d_1 = x_n^2(x_{n+2} - x_{n+1}) - x_{n+1}^2(x_{n+2} - x_n) + x_{n+2}^2(x_{n+1} - x_n)$$
$$e_1 = x_n(z_{n+1}^2 - z_{n+2}^2) + x_{n+1}(z_{n+2}^2 - z_n^2) + x_{n+2}(z_n^2 - z_{n+1}^2)$$

Expression 10 is not valid in the case that $x_n=x_{n+1}=x_{n+2}$. For this particular case, another similar equation (expression 11) is obtained by following the same procedure, but obtaining and equalling z_p instead of x_p from expressions 6 and 7. As in expression 10, this expression is not valid when $z_n=z_{n+1}=z_{n+2}$.

$$a_2 r_n^2 - b_2 r_{n+1}^2 + c_2 r_{n+2}^2 = d_2 + e_2 \qquad (11)$$

being in this case

$$a_2 = (z_{n+2} - z_{n+1})$$
$$b_2 = (z_{n+2} - z_n)$$
$$c_2 = (z_{n+1} - z_n)$$
$$d_2 = x_n^2(z_{n+2} - z_{n+1}) - x_{n+1}^2(z_{n+2} - z_n) + x_{n+2}^2(z_{n+1} - z_n)$$
$$e_2 = z_n(z_{n+1}^2 - z_{n+2}^2) + z_{n+1}(z_{n+2}^2 - z_n^2) + z_{n+2}(z_n^2 - z_{n+1}^2)$$

To obtain the discriminating functions, it is only necessary to include the distances r_i (with $0 \le i \le 8$) in expressions 10 and 11 according to the times-of-flight corresponding to the two types of basic reflector (expressions 1 and 2). For this purpose, the transducers are arranged in groups of three elements, as shown in table I. Expressions 10 and 11 are applied to each group according to their position, so that if the three sensors are located on the x axis, it is only possible to apply expression 10 to them. In the case that they are located on the z axis, only expression 11 is applied to them. In every other case both expressions are applied to them.

Group	Transducers	Expressions applied	Discriminating functions
1	S0, S1 ,S2	10	fs1, fm1
2	S0, S3, S4	11	fs2, fm2
3	S0, S6, S7	10 11	fs3, fm3 fs4, fm4
4	S0, S5, S8	10 11	fs5, fm5 fs6, fm6

Table I. *Groups of sensors and discriminating functions*.

Six discriminating functions are obtained for edges and another six are obtained for planes (table II).

Group	Discriminating Functions
1 $n=S0$ $n+1=S1$ $n+2=S2$	$fs1 = \frac{a_1}{4}t_{00}^2 - b_1(t_{01} - \frac{t_{00}}{2})^2 + c_1(t_{02} - \frac{t_{00}}{2})^2 = \frac{d_1 + e_1}{c} = K1$ $fm1 = a_1 t_{00}^2 - b_1 t_{01}{}^2 + c_1 t_{02}{}^2 = \frac{d_1 + e_1}{c} = K1$
2 $n=S0$ $n+1=S3$ $n+2=S4$	$fs2 = \frac{a_2}{4}t_{00}^2 - b_2(t_{03} - \frac{t_{00}}{2})^2 + c_2(t_{04} - \frac{t_{00}}{2})^2 = \frac{d_2 + e_2}{c} = K2$ $fm2 = a_2 t_{00}^2 - b_2 t_{03}{}^2 + c_2 t_{04}{}^2 = \frac{d_2 + e_2}{c} = K2$
3 $n=S0$ $n+1=S6$ $n+2=S7$	$fs3 = \frac{a_1}{4}t_{00}^2 - b_1(t_{06} - \frac{t_{00}}{2})^2 + c_1(t_{07} - \frac{t_{00}}{2})^2 = \frac{d_1 + e_1}{c} = K3$ $fm3 = a_1 t_{00}^2 - b_1 t_{06}{}^2 + c_1 t_{07}{}^2 = \frac{d_1 + e_1}{c} = K3$ $fs4 = \frac{a_2}{4}t_{00}^2 - b_2(t_{06} - \frac{t_{00}}{2})^2 + c_2(t_{07} - \frac{t_{00}}{2})^2 = \frac{d_2 + e_2}{c} = K4$ $fm4 = a_2 t_{00}^2 - b_2 t_{06}{}^2 + c_2 t_{07}{}^2 = \frac{d_2 + e_2}{c} = K4$
4 $n=S0$ $n+1=S5$ $n+2=S8$	$fs5 = \frac{a_1}{4}t_{00}^2 - b_1(t_{05} - \frac{t_{00}}{2})^2 + c_1(t_{08} - \frac{t_{00}}{2})^2 = \frac{d_1 + e_1}{c} = K5$ $fm5 = a_1 t_{00}^2 - b_1 t_{05}{}^2 + c_1 t_{08}{}^2 = \frac{d_1 + e_1}{c} = K5$ $fs6 = \frac{a_2}{4}t_{00}^2 - b_2(t_{05} - \frac{t_{00}}{2})^2 + c_2(t_{08} - \frac{t_{00}}{2})^2 = \frac{d_2 + e_2}{c} = K6$ $fm4 = a_2 t_{00}^2 - b_2 t_{05}{}^2 + c_2 t_{08}{}^2 = \frac{d_2 + e_2}{c} = K6$

Table II. Discriminating functions.

In the theoretical case of an absence of noise in the measurements, the calculation of the previous expressions will unequivocally ascertain the type of reflector, given that for each discriminating function the following will be fulfilled:

$$\begin{gathered} \text{If} \;\; fmi - Ki = 0 \Rightarrow Wall \\ \text{If} \;\; fsi - Ki = 0 \Rightarrow Edge \end{gathered} \qquad (12)$$

When, under real circumstances, the measurements are contaminated by certain levels of noise:

$$\begin{gathered} (fmi - Ki)^2 = \varepsilon_{mi}^2 \\ (fsi - Ki)^2 = \varepsilon_{si}^2 \\ \text{If} \;\; (\varepsilon_{si}^2 - \varepsilon_{mi}^2) > 0 \Rightarrow wall \;\; type \;\; reflector \\ \text{If} \;\; (\varepsilon_{si}^2 - \varepsilon_{mi}^2) < 0 \Rightarrow edge \;\; type \;\; reflector \\ \text{If} \;\; (\varepsilon_{si}^2 - \varepsilon_{mi}^2) = 0 \Rightarrow undefined \;\; reflector \end{gathered} \qquad (13)$$

One of the principal contributions of the sensor structure presented here is that, by having several measurements simultaneously available, a high level of redundancy is produced so that when erroneous measurements occur in one of the transducers, classification is barely affected as the final decision is reached via voting techniques between the six discriminating functions.

5. Results.

To refine and check the operation of the proposed algorithm, a simulator has been developed that enables the times-of-flight measured by each transducer to be obtained for wall and edge-type reflectors situated at various locations within the three-dimensional space. In this simulator, the errors that affect the measurements taken by ultrasonic sensors have been statistically modelled using a Gaussian distribution function [17,19] of null average and standard deviation determined by the characteristics of the environment and by those of the transducer itself (mechanical and electronic).

Figure 6 shows the values of discriminating functions fs_i and fm_i ($1 \leq i \leq 6$) obtained for a series of ideal TOF (without additional noise) for a edge-type reflector and for distances ranging from 25 to 600 cm. As may be observed, the value of fs remains constant and equal to k_i, whilst that of fm_i varies until it stabilises at a value of approximately $2*k_i$.

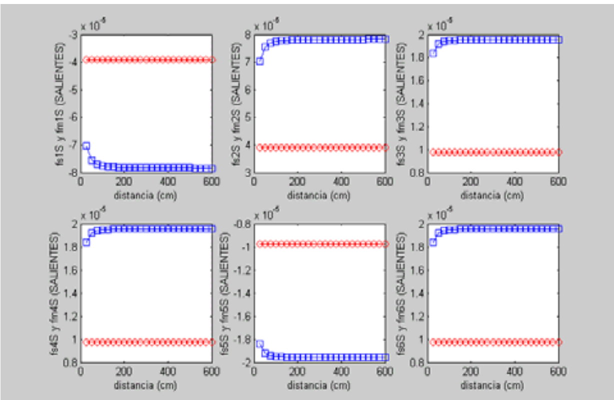

Fig. 6. Functions fs_i and fm_i for edge-type reflectors.

Figure 7 shows the function delta=(ε_{s1}^2-ε_{m1}^2) for the case of a plane-type reflector. Errors have been added to the TOF ranging from 5 to 20µs. As may be observed, in the absence of noise delta>0, which means that the classification algorithm would clearly indicate that it is a plane-type reflector. As the noise is increased in the measurements, delta approaches zero and even takes positive values from 4 metres onwards in the case of added noise of 5 µs, and from 2 metres onwards in all other cases.

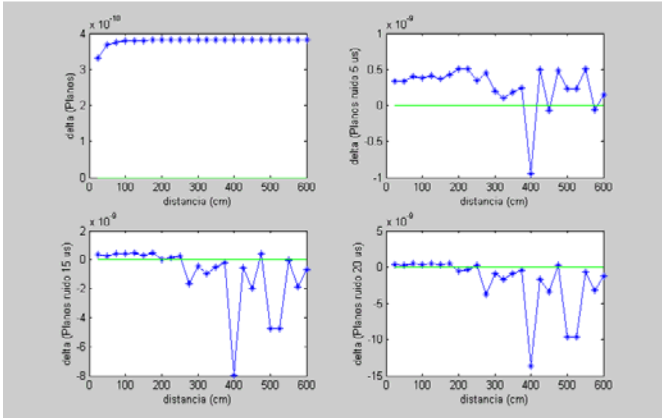

Fig. 7. Function delta=(ε_{s1}^2-ε_{m1}^2) for plane-type reflectors for TOF contaminated by varying levels of noise.

6. Future Works.

The classification algorithm is currently being extended so that, as well as classifying planes and edges, it is also able to classify corners. As is known, in order to be able to differentiate between corners and planes it will be necessary to make at least two emissions. For this purpose the complete structure shown in figure 1 is used.

Attempts are also being made to improve the classification algorithm, although a more complex calculation would be required to make the classification more robust when the distances exceed the indicated limit of 2.5 metres.

Acknowledgements

The work described in this paper was made possible by funding for the TELEVIA (COO1999-AX049) research project by the Ministry of Science and Technology of Spain.

References.

[1] Kleeman L., Kuc R., “Mobile Robot Sonar for target localization and classification”. The International Journal of Robotics Research. Vol.14, nº4. pp. 295-318. 1995.

[2] Wijk, O., Christensen, H.I., “Triangulation-based fusion of sonar data with application in robot pose tracking”, IEEE Transactions on Robotics and Automation, Vol: 16, Issue: 6 , pp:740-752, 2000

[3] Lim J. H., Cho D. W., “Experimental investigation of mapping and navigation based on certainty grids using sonar sensors”, Robotica (UK), vol.11, pp. 7-17, 1993

[4] Matthies L., Elfes A., “Integration of sonar and stereo range data using a grid-based representation”, Proc. of the 1988 IEEE Int.Conf. on Robot. and Aut., Philadelphia, vol.2, pp. 727-733, 1988.

[5] Pagac D., Nebot E.M., Durrant-Whyte H., “An evidential Approach to Map-Building for Autonomous Vehicles”, IEEE Trans. on Robot. and aut., vol.14, no.14, pp. 623-629, Agosto 1998

[6] Oriolo G, Ulivi G., Vendittelli M., “Motion planning with uncertainty: navigation on fuzzy maps”, *Proc*. 4th. IFAC Symp. on Robot Control, Capri, I, pp. 71-78, 1994.

[7] Van Dam J.W.M., Kröse B.J.A., Groen F.C.A., “Neural Network applications in sensor fusion for an autonomous mobile robot”, Proc. Int.wokshop on Reasoning with Uncertainty in Robotics, pp.1-19, 1996

[8] Gambino F., Oriolo G., “A comparison of three uncertainty calculus techniques for ultrasonic map building”, SPIE Int. Symp. Aerospace/Defense Sensing Contr., pp. 249-260, Orlando 1996,

[9] V. Díaz, J. Ureña, M. Mazo, J. J. García, E. Bueno, and A. Hernández, “Using complementary sequences for multi-mode ultrasonic operation”, in Proc. 7th IEEE International Conference on Emerging Technologies and Factory Aut. (ETFA’99), pp. 599-604, Barcelona, 1999

[10] Barshan, B. and Kuc R., “Differentiating sonar reflections from corners and planes by employing an intelligent sensor”, IEEE Transactions on Pattern Analysis and Machine Intelligence, vol.12, No.6, pp. 560-569, 1990.

[11] Barshan B., Ayrulu B., Utete W., “Neural network-based target differentiation using sonar for robotics applications”, IEEE Trans. on Rob. and Automation. vol:16, no4. pp. 435-442, 2000.

[12] Hong M. L.; Kleeman, L.” A low sample rate 3D sonar sensor for mobile robots ”. Proceedings of the 1995 IEEE International Conference on Robotics and Automation, Vol: 3 , pp.: 3015 -3020. 1995.

[13] Akbarally H., Kleeman L., “A sonar sensor for accurate 3D target localisation and classification”, IEEE lnt. Conf. on Robot. and Aut., Nagoya (Japón), , pp. 3003-3008, 1995.

[14] Watanabe S., Yoneyama M., “An ultrasonic visual sensor for three-dimensional object recognition using neural networks”, IEEE Trans. on Robot. and aut., vol.8, no.2, pp. 240-249, 1992.

[15] Knoll, A.C., “Ultrasonic holography techniques for localizing and imaging solid objects”, IEEE Transactions on Robotics and Automation. Vol: 7, pp: 449 -467. 1991.

[16] Acampora A.S., Winters J.H., “Three-dimensional ultrasonic vision for robotic applications”, IEEE Trans. Pattern Anal. Machine Intell., vol.11, no.3, pp. 291-303, 1989.

[17] Ureña J., “Contribucción al diseño e implantación de un sistema sonar para la automatización de un vehículo industrial”. Ph. thesis. Electronic Department. Alcala University. 1998.

[18] A. Hernández, J. Ureña, J. J. García, M. Mazo, J. P. Dérutin, J. Serot. “Ultrasonic sensor performance improvement using DSP-FPGA based architectures”. 28th IEEE International Annual Conference on Industrial Electronics, Control and Instrumentation (IECON'02),.pp. 2694-2699, Seville, 2002.

[19] Kuc R., Siegel M.W. “Physically Based Simulation Model for Acoustic Sensor Robot Navigation”. IEEE Transactions on Pattern Analisys and Machine Intelligence. Vol. 9, nº 6, pp. 766-778. Noviembre 1987.